resources

MDPI

Article

New Lime-Based Hybrid Composite of Sugarcane Bagasse and Hemp as Aggregates

Arlen Zúniga [1,*], Rute Eires [1,2] and Raphaele Malheiro [2]

[1] Department of Civil Engineering, University of Minho, 4800-058 Guimarães, Portugal
[2] Centre for Territory, Environment and Construction (CTAC), University of Minho, 4800-058 Guimarães, Portugal
* Correspondence: lizethnic@yahoo.com.ar

Abstract: Bio-based materials help reduce the consumption of non-renewable resources, contributing to the development of sustainable construction. Industrial Hemp Concrete (IHC), which uses hemp stalk (HS) as an aggregate and a lime-based binder, is a bio-based material with various applications. This research developed a new hybrid composite in order to improve the mechanical strength and durability of hemp concrete, with the incorporation of sugarcane bagasse (SCB) as an aggregate, a resource of a renewable origin that is abundant in several countries. Different formulations were used, which were molded and pressed manually, evaluating their cohesion and compactness. The performance of the developed hybrid composite was measured considering mechanical, thermal, and-durability properties. The compression test results showed an increase of 19–24% for composites with 75% hemp and 25% SCB. Thermal conductivity and thermal resistance coefficients were also improved, reaching 0.098 (W/m °C) and 0.489 (m^2 °C/W), respectively. This aggregate combination also showed the lowest water absorption coefficient (reducing by 35%) and the best performance in durability tests compared to IHC. The resistance to freeze–thaw is highlighted, increasing 400%. The main reason is the influence of the SCB addition because the short and thin fiber form helps to maintain the physical integrity of the composite by filling the spaces between the hemp aggregates.

Keywords: hemp concrete; sugar cane bagasse; new composite; sustainability; durability

Citation: Zúniga, A.; Eires, R.; Malheiro, R. New Lime-Based Hybrid Composite of Sugarcane Bagasse and Hemp as Aggregates. *Resources* **2023**, *12*, 55. https://doi.org/10.3390/resources12050055

Received: 23 March 2023
Revised: 15 April 2023
Accepted: 17 April 2023
Published: 27 April 2023

1. Introduction

The construction sector plays a major role in the CO_2 emissions produced by all activities related to the construction process (around 40%) [1]. Therefore, it is necessary to look for alternative materials, technologies, and construction methods that significantly reduce the consumption of resources and energy by providing better energy efficiency without causing pollution and harming health and ecosystems. In this sense, plant components could be used as a possible input to lighten concrete mixes [2].

Since the early nineties, a new building material was obtained by mixing hemp particles (the fibrous non-fraction of the hemp stalk called ''hurds''), and a lime-based binder was developed. This allowed for the construction of sustainable buildings (for the construction of new buildings or the renovation of existing buildings) as a filler material for a load-bearing structure [3]. Since then, Industrial Hemp Concrete (HC) has been widely studied in construction as a versatile bio-based material option; it is "carbon-negative" because the hemp plant absorbs more carbon from the atmosphere than it emits during its production and application on site [4] and captures carbon through the carbonation process of lime. According to Jami et al. [5], it is a cellulosic aggregate concrete using hemp as aggregate and a lime-based binder, which could be referred to as cellulosic aggregate concrete.

However, small changes in its composition and manufacturing process can cause many variations in the product result, which can be a barrier to widespread its utilization [4]. Its long-time performance is another concern about this type of composite, namely, under extreme temperature variation and saline exposure [6].

There are very few studies that focus on increasing the mechanical performance of hemp concrete. Currently, only the mechanical characterization of hemp concrete is being investigated [4]. Therefore, this study aims to present an alternative to improve the performance not only from the mechanical point of view but also from its durability with the addition of agro-industrial wastes, similar to hemp–lime concrete; other agro-residues have also been tested in lime-based mixtures: sunflower stalk [7,8]; rice [9]; miscanthus [10]; flax [11]; and flax mixed with hemp [12]. In this study, we are considering sugar cane bagasse and sugar cane ash.

These agro-industrial wastes have been studied as a fiber to improve the strength and durability of earth blocks [13,14] and clay bricks [15] and as a partial substitute for Portland cement, in applications such as high performance concrete [16] or as a substitute for common concrete, by evaluating its durability [16–19] and endorsing its pozzolanic performance [20,21].

Studies such as Murphy et al. studied [22] how to optimize the properties of IHC by testing hydrated lime and a commercial binder with different ratios (25, 50, 90%) and their influences on the mechanical behavior. Their results showed that the compressive strength increased with the binder content. Araújo (2015) [23] studied different percentages of hydrated lime, reaching good mechanical results with a proportion of 70% hydrated lime, with 0.60 Mpa in compressive strength.

Walker et al. (2014) [6] focused on the relationship between the type of binder and the mechanical resistance and durability of the proposed mixtures. Good results were obtained in the freeze–thaw tests, where the compositions with higher amounts of hydraulic binders (66.6%) decreased their water absorption capacity and were, therefore, less affected by temperature variations and the low incidence of salts due to the high ductility of the pore walls of hemp, which adapt to the expansive pressures of salt crystallization.

SCB is a residue from the production process of sugar and its derivatives, present in several countries, with an average annual production of 1,889,268,880 tons, where the main world producer is Brazil [24]. In 2018 alone, Brazil produced 746.8 million metric tons of sugarcane, followed by India with 376.9 million metric tons and China with 108.7 million metric tons, with an estimated production of over 400 million metric tons of SCB [25]. In 2017, the US produced 28.0 million metric tons of sugarcane, mainly in Florida, Louisiana, and Texas [26], producing approximately 9 million metric tons of SCB. Only about half of the SCB produced is used for power generation in the sugar mills, while the remaining part is disposed of in landfills, creating environmental problems and a potential fire hazard [13]. In this study, we use the SCBA that comes from Nicaragua, which ranks 25th, producing 7,351,391. 58 MT of sugar and 1,940,767.38 MT of residues [27].

The high productivity of agricultural crops is the main reason for the large volume of agricultural waste [28]. At this time, those wastes are either burned or landfilled, causing multiple problems such as air pollution, greenhouse gas emissions, and inappropriate land use [29]. As such, research into new uses for agro-residues in different applications has been growing, and construction is one of them. In conventional cement-based concrete, it has been used to partially replace aggregates [30] or for reinforcement as a fiber, similar to synthetic fibers [31,32].

The abundance of residual SCBA produced each year and the problems associated with waste disposal promote interest in valorizing this agricultural by-product by identifying new beneficial applications. In fact, sugar cane juice extraction produces a large volume (32%) of SCBA as a waste product [33,34]. Considering the issues of agricultural waste incineration in a controlled environment is a method that reduces the pollution associated with uncontrolled open burning. Controlled biomass burning contributes to

generating steam energy for electricity generation in developing countries, and the residual ash produced in this process can be reused [35].

Therefore, considering the chemical and physical properties of agricultural waste ash (AWA) and its worldwide availability, the effective use of alternative cementitious materials in large quantities is recommended. In this way, the environmental impact can be further reduced by reducing clinker production and the open burning of agricultural waste [36]. The availability of bagasse ash is very high, as can be seen from the statistics, for use as alkali activated binder precursors or as a blending material in cement production [21].

For this reason, we also take Souza's study [37]. SCB, in combination with lime as a binder, showed the best results in terms of mechanical strength; 0.495 MPa of maximum compressive strength and 0.76 MPa of flexural strength were obtained with the lime addition, with a composition of 30 to 35% SCB and 70 to 65% lime, experimenting also with other materials such as soil and binders such as metakaolin in combination with lime. Additionally, Kumar et al. [13] added SCB as a fiber for soil blocks, and the authors concluded that stabilized soil blocks containing 0.5% or 1.0% by weight of SCB and 12% by weight of cement provided the best compromise between strength and durability, meeting the recommendations corresponding to the design standards, representing a promising solution for the construction of affordable, ecological, and low-rise housing.

With respect to SCBA studies, such as from Charitha et al. [34], we characterize it with high pozzolanic capacity due to its high content of SiO_2, $Al2O_3$, and Fe_2O_3, totaling more than 70%, classified according to ASTM C618, proving its effectiveness in studies from Dineshkumar [16], Vasudha [17], and Bahurudeen [38] where SCBA was partially added in proportions between 20 and 30% to replace the role cement with cementitious material, evaluating the durability properties, such as water absorption, carbonation, and corrosion resistance. The results obtained showed adequate support to the replacement.

In the present study, based on the master's thesis of Zúniga [39], in the search for improvement of mechanical properties and durability of the hempcrete (IHC), the combination of industrial hemp (IH) and sugar cane bagasse (SCB) as an aggregate was studied. Different formulations were made with the addition of binders such as hydrated lime, brick dust, and sugarcane bagasse ash (SCBA) to evaluate their behavior in terms of mechanical properties, thermal behavior, and durability.

2. Materials and Methods

2.1. Materials

The hemp used was a commercial crushed and pre-corticated hemp stem (also known as shiv), cultivated and processed in France by the Chanvrière de I`Aube (LCDA) company. Its physical and chemical properties, according to the technical data sheet provided by the manufacturer, can be seen in Table 1. No pretreatment was carried out for its application. The length of hemp used varied mainly between 10 and 20 mm, with diameters ranging mainly from 1 to 4 mm.

Table 1. Physical and chemical properties of the hemp aggregate.

Characteristic	Measurement
Density	100 to 110 kg/m^3 (depending on relative humidity), loosely packed, not compressed
Water absorption	198%
Water absorption of mineral elements	24 mEq per 100g of raw material
Calorific value	3804 cal/g
Thermal conductivity (10 °C in a dry state)	0.0486 W/m.K
Water	9 to 13%
Dry material	85 to 90% of which
Total organic material	97.5% on a dry basis of which:
Net cellulose:	52%
Lignin:	18%
Hemicellulose:	9%
Minerals	Calcium: 1% on a dry basis Magnesium: 0.03% on a dry basis Phosphorus: 9 mg/100 g Potassium: 0.8% on a dry basis Total nitrogen: 0.4 to 1% on a dry basis Total carbon: 496 g/kg on a dry basis C/N: 87 Ash: 2% pH in suspension at 10%: 6.7

The sugar cane bagasse used, of the Yuba variety, from Madeira Island, at the sugar mill, was subjected to a milling process in a 3-cylinder mill; in the laboratory, it was only air-dried (20 °C and 50% RH), and no treatment was applied. See Figure 1.

(**a**) (**b**)

Figure 1. (**a**) Hemp without any further treatment. (**b**) Sugar cane bagasse from Madeira Island, without any additional treatment.

The length of SCB varied between 10 and 30 mm, but most were close to 15 mm, with diameters ranging from 0.2 to 0.5 mm. SCB was typically constituted by cellulose (50%), hemicellulose (25%), and lignin (20%) [37]. However, its chemical composition could also be observed by analyzing its ash (SCBA), as shown in Table 2. It was mainly composed of silica, iron, aluminum, and calcium.

The lime used was calcium hydroxide or calcic lime, CL (commonly known as slaked or hydrated lime), named Lusical H100 (CL 90-S), with more than 80% free lime and 5% magnesium oxide, which is for construction and civil engineering applications or materials. As a complement, SCBA was used as pozzolan. It is a residue from the production of

sugar and honey by the Montelimar Corporation through its cogeneration plant Green Power S.A. for the generation of clean electricity from biomass. Brick dust (BD) from construction waste was also used, which was processed at the Construction Materials Laboratory of the University of Minho. It is important to highlight that we sought to use materials with a low environmental impact, which was why cement and mineral aggregates have not been included in the studied compositions. In Figure 2, there is the presentation of the lime used (CL) and the two additional binders added, sugar cane bagasse ash (SCBA and brick powder (BD) and Table 2 shows the chemical composition of these.

(**a**) (**b**) (**c**)

Figure 2. (**a**) Hydrated lime (CL). (**b**) Sugar cane bagasse ash (SCBA. (**c**) Brick powder (BD).

Table 2. Chemical composition of binders.

Components	CL	SCBA	BD
SiO_2 (%)		54.13	58.83
$Al2O_3$ (%)		10.61	25.39
Fe_2O_3 (%)		12.553	7.92
CaO (%)		10.852	0.5
MgO (%)	≤5	0.324	1.59
TiO_2 (%)		0.919	1.22
P_2O_5 (%)		3.606	
SO_3 (%)	≤2		
MnO (%)		0.324	
Na_2O (%)			0.42
K_2O (%)		6.292	4.13
Cu		0.04	
Zn		0.052	
Sr		0.155	
LOI (%)			
CO_2	≤4		
Cal Livre	≥80		
CaO + MgO	≥90%		

2.2. Compositions

To select the reference mixtures of hemp concrete, different studies were considered, indicating better mechanical results with the use of lime [23,40] in a hemp/lime ratio of 25–75% to 30–70% by mass, respectively.

Based on a previous experimental process carried out in the laboratory and the references studied in the state of the art, 8 mixtures with the best compressive strength results, considering the lower percentage of lime. It began to be used a 25/75% aggregates/binders ratio, after a 30/70% ratio in order to try a binder reduction. However, for better results, a 25/75% ratio was used in the last mixture. The lime amount was also reduced with a partial substitution of other binders. The mixes that were combined with the two additional binders (BD-SCBA) and the mechanical strength performance improved

with the different % addition of SCB to the hemp concrete. The mixtures only with brick dust (BD) or with SCB ash (SCBA) were tested to evaluate the adhesion of these materials with the aggregates and their isolated performance in terms of resistance and durability. The last mixture use lime and SCBA without BD since no advantages were found in the addition of this material.

Table 3 identifies and shows the mixtures studied. The mixes identification is according to the materials abbreviations with the initial letter of the binder.

Table 3. Mixing performed.

Mix	Total Aggregates/ Binders Ratio (%)	Aggregates		Binders		
		Hemp (%)	SCB (%)	Hydrated Lime	BD	SCBA
H-L-ref	25/75	100		100		
HS-L	25/75	75	25	100		
HS-B	25/75	75	25		100	
HS-A	25/75	75	25			100
HS25-L-B-A	30/70	75	25	50	25	25
HS50-L-B-A	30/70	50	50	50	25	25
HS75-L-B-A	30/70	25	75	50	25	25
HS-L-A	25/75	75	25	75		25

2.3. Methods Applied

The procedures of the mixture preparation were based on Murphy et al.'s [22] research, where no pre-treatment of hemp wetting was carried out since they did not contribute significant benefits to the properties. The binders were mixed in their powder presentation, and then a part of water was added until a pasty consistency was obtained. Then, the aggregates were added gradually, until the paste covered the aggregates during an average mixing time of 6 min, evaluating the consistency of the mixture with the manual elaboration of a ball. If the ball maintained the shape and presented good cohesion, it meant that the workability of the material was adequate to produce the specimens, as has been used by Sousa to aid in the verification of the adhesion of materials [37], see Figure 3.

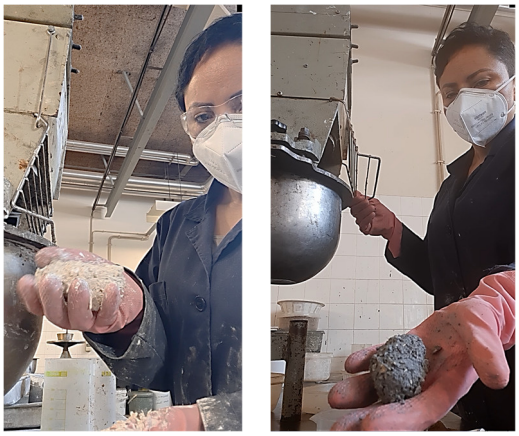

(**a**) (**b**)

Figure 3. Example of boll for evaluation of mixtures. (**a**) Ball of H-L-ref. (**b**) ball of HS-L-A.

It was then placed in oiled-prior metal molds, lightly pressed, and vibrated for 40 sec. After 24 h of curing (20 °C and 50% RH), it was removed from the molds and placed in a laboratory environment (20 °C and 50% RH) for 28 days. The molds were prepared in

measurements of 40 × 40 × 160 mm, 50 × 50 × 50 mm, and 150 × 150 × 50 mm, according to the requirements of the different tests that were carried out.

2.3.1. Compressive Strength Performance

In the case of hemp concrete, there are no standards to evaluate its mechanical resistance. This study takes the BS EN 1015-11 2019 [41] (Compression) standard. Adjusting the conditions of the material with an application of 20N/s by displacement of the force applied on the specimen until the rupture of the same. For the application of this test, specimens of 50 × 50 × 50 mm were tested with a curing time of 28 days (3 specimens for each mixture). The Figure 4 shows the specimens before the test and one during the test.

(**a**) (**b**)

Figure 4. (**a**) Samples; (**b**) disposal for compression test in the Lloyd-LR50K.

2.3.2. Thermal Conductivity Test

The Prototherm prototype [42] was used to evaluate the thermal properties. The methodology followed for this test was the internal procedure of the LMC (Laboratory of Construction Materials of the Department of Civil Engineering of the University of Minho), adapted from ISO-9869-1994 [43]. Figure 5 shows the prototherm with the heat source and a specimen to be evaluated. The test consists of placing a heat source and heat sink at the trapezoidal end towards a 60 cm wide rectangular section. Temperature sensors were arranged to measure the temperatures of the environment, the heat source, the heat sink, and the two internal environments: internal channel 1 and 2.

(**a**) (**b**) (**c**)

Figure 5. (**a**) The prototherm prototype. (**b**) internal channel 1. (**c**) internal channel 2.

In this test, the heat source was set to 200 °C to obtain an average internal inlet channel temperature of 39–40 °C constant for 24 h. For the application of this test, one sample of 150 × 150 × 50 mm per mix was tested with a curing time of 60 days because a higher percentage of carbonation had already occurred.

2.3.3. Coefficient of Water Absorption by Capillarity

The capillarity test was performed in accordance with BS EN 1015-18 [44] and C 1585-04 [45] for the determination of the capillary water absorption coefficient of hardened concrete and for the measurement of the water absorption rate of hydraulic concrete, taking into account the materials characteristics of in this study.

As a preliminary procedure, the samples were subjected to a period of drying in an oven at 60 °C, until a constant mass, after which a silicone coating was applied on the lateral faces, leaving only the upper and lower faces free, the latter being exposed to a humid surface. Weight control was carried out on a time scale until constant values were reached in the defined period. For the application of this test, the dimensions of the samples were 50 × 50 × 50 mm, with a curing time of 60 days (3 specimens for each mixture), see Figure 6.

(**a**) (**b**)

Figure 6. (**a**) prepared samples; (**b**) capillary absorption test (samples on water saturated oasis).

2.3.4. Freezing and Thawing Resistance

For hemp concrete, there is no standard for the application of this type of test; thus, ASTM C 666/C 666M-03 [46] was followed, adapting it to the material conditions. Previously, the mixtures were subjected to a mass control to characterize the initial conditions of the samples. In the freeze–thaw chamber, the samples were placed on a surface that allowed contact with water on only one side of the sample, with a water level of 15 mm, to produce the absorption effect of the fibers, considering that it is an outdoor side that is generally exposed to climatic variations.

The samples were subjected to freezing and thawing cycles of 21,600 s for each cycle, and, in Figure 7, you can see the chamber used in the process until the specimen was visibly destroyed, for which 24 h visual controls were carried out. For the application of this test, the dimensions of the samples were 50 × 50 × 50 mm, being 3 specimens per mixture, with a curing time of 60 days.

(**a**) (**b**)

Figure 7. (**a**) Control panel; (**b**) specimens in freezing–defrosting chamber.

2.3.5. Degradation by Exposure to Simulated Rain

Considering the characteristics of the materials in this study, the accelerated test proposal of Rezende et al. [47] was used to evaluate the degradation by rain simulation. The exposure time (5 h) was the equivalent of 100 years, with mass recording before and after the test to calculate the percentage of rain absorption and erosion wear.

The effects were assessed by a mechanical flexural strength test, according to BS EN 1015-11 2019 (Flexure) [41], compared to samples that had not been subjected to this simulation, in addition to a weight control before and after the test. For the application of this test, the dimensions of the specimens were 150 × 150 × 50 mm, with 3 specimens for each mixture, with a curing time of 60 days. A coating of a dry mortar formulated from natural hydraulic lime was applied. Figure 8 shows the test process.

(**a**) (**b**)

Figure 8. (**a**) Rainfall degradation simulation test process. (**b**) flexural test after samples are subjected to rain degradation process (Lloyd-LR50K).

2.3.6. Saline Exposure

The salt exposure test was performed in accordance with BSI 3900-F2 1973 [48] for the determination of resistance to moisture, for the neutral salt test, adjusting the procedures to the type of material.

The cure time of the samples was 28 days, and the exposure time was 60 days. The temperature range of the experiment was between 24 and 48 °C, with cycles of 24 h to subject the samples to the vapor of the liquid medium previously prepared, in 1.5 L of drinking water and 200 gr of coarse salt.

The method to evaluate the effect of the salt vapor consisted of testing the mechanical resistance to compression, taking up the BS EN 1015-11 2019 [41] standards (compression), and comparing the results with those of the samples that were not subjected to this test with the same curing time. Weight control was performed at the beginning and at the end of the test. For the application of this test, the dimensions of the specimens were 50 × 50 × 50 mm, with 3 specimens per mixture, see Figure 9.

Figure 9. Temperature-controlled salt vapor preparation process.

3. Results: Strength and Durability of the New HC-SCB Composite

3.1. Compositions (Fresh State)

The fresh state of the mixtures, shown in Table 3, was visually evaluated using an optical microscope (indicate magnification). Figure 10 shows the images of the eight mixes, in their fresh state, which allowed for the observation of spaces between the fibers, the integration, and the coating of the binders on the aggregates.

In the HL-ref concrete composition (Figure 10a), the hydrated lime adhered to the hemp particles and filled the spaces between them, making the mixture more cohesive. It was found that it was visible when there was greater coverage of the aggregates because there was better adhesion of the binder to these, and they provided better cohesion in the mixtures and in filling the voids. In the formation of the new composite, SCB pieces filled these spaces and bonded the hemp shavings together, creating a network between the spaces. It was also noted that the BD did not mix homogeneously with the rest of the binders, presenting small concentrations of BD (Figure 10c, f–h).

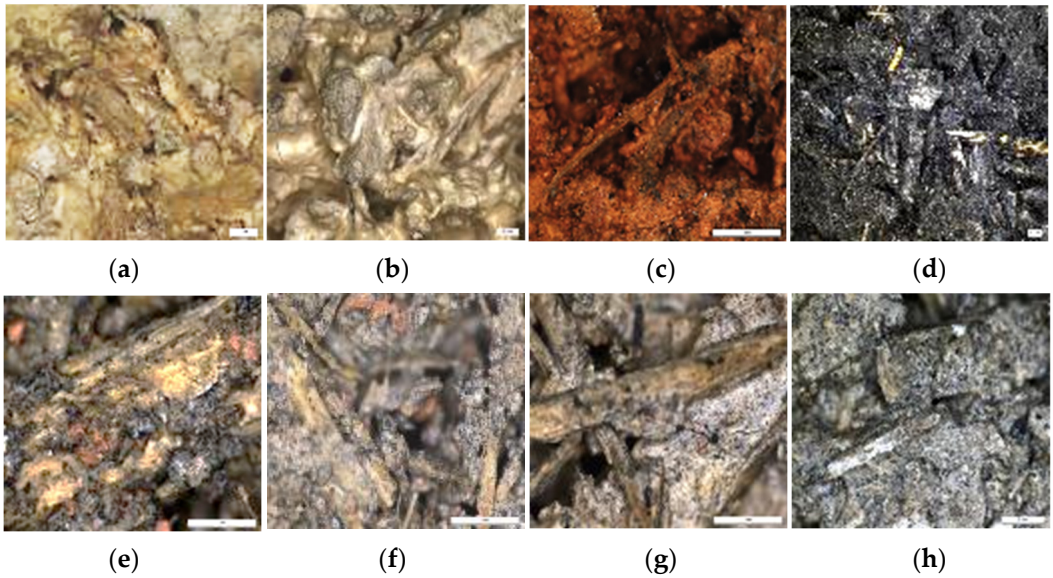

Figure 10. Microscopic images zoom 6x: (**a**) H-L-ref. (**b**) HS-L. (**c**) HS-B. (**d**) HS-A. (**e**) HS25-L-B-A. (**f**) HS50-L-B-A. (**g**) HS75-L-B-A. (**h**) HS-L-A.

3.2. Compressive Strength Performance

Figure 11 shows the compressive strength results for the mixtures. Considering the reference situation (HL-ref), one can observe that there is no loss in the mechanical resistance only with two mixtures, HS-L and HS-L-A. Furthermore, they provide an

improvement in the performance of the mixtures, highlighting the pozzolanic efficiency of the SBA addition in this type of composite. In these mixtures, the HS-L mixture reached 0.41 MPa, almost 25% more than the HL-ref, 0.33 MPa. For the HS-L-A, the increase in the compressive resistance is higher than the HS-L. The HS-L-A mixture reaches 0.46 MPa, almost 39.39% than the HL-ref. It is important to note that there was a reduction of 25% in the hydrated lime used in the last case, HS-L-A, since this percentage was replaced by SCBA (while in the HS-L the binder is only the hydrated lime). The reduction in the hydrated lime content is an important achievement since it promotes a more sustainable material.

The satisfactory performance in composites based on lime was already shown in other research [23,40,49,50], with an average compressive strength of 0.48 MPa, which meant that that there was a better compressive strength at a proportion of more than 70% of the binder.

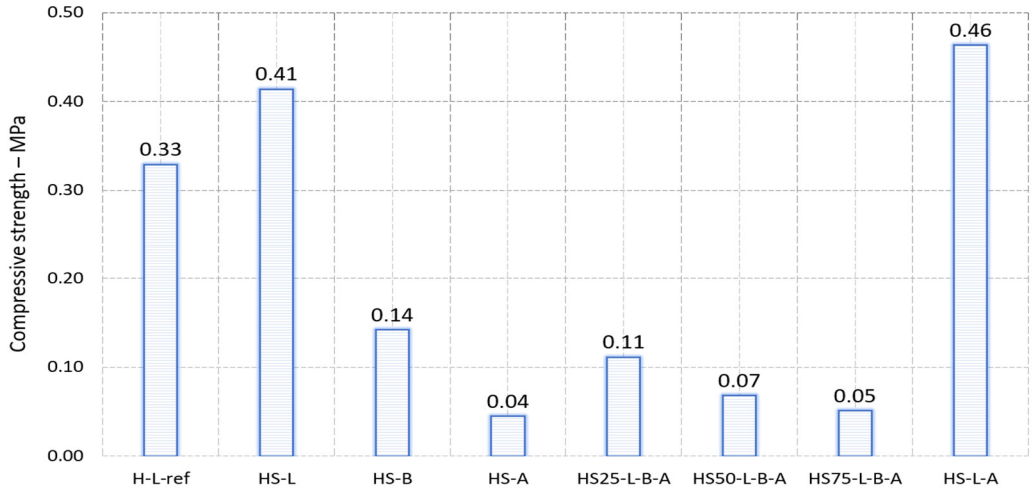

Figure 11. Compressive strength.

In the mixtures where there was no hydrated lime as binder, HS-B and HS-A, there was a sharp drop in the compressive strength, which, in a certain way, was already expected since pozzolanic materials were effectively efficient when combined with calcium hydroxide [51]. Considering the mixtures that used three different binders (hydrated lime, brick dust, and ash) and aggregates (hemp and SCB) divided in different ratios (with 25, 50, and 75% of SCB), it could be seen that the higher the addition of SCB the lower the resistance. In addition, the compressive strength was unsatisfactory, varying between 0.05 and 0.11 MPa. Figure 12 shows the state of the test specimens after the application of the compression test.

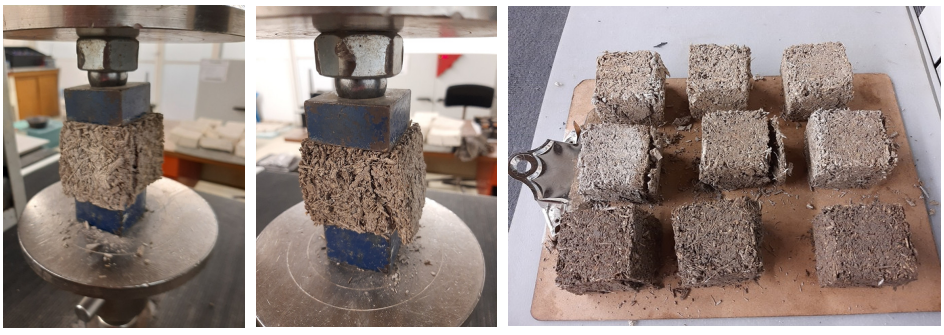

(**a**) (**b**) (**c**)

Figure 12. Samples subjected to compression test: (**a**) and (**b**) during the text; (**c**) after the test.

In other study, it was also shown that brick dust did not improve the mechanical properties of hemp concrete, as concluded by Sinka and Sahmenko (2013) [52] in their study using hemp composites with hydraulic lime and ground brick as pozzolanic mix. It showed little hydraulic activity and could only be used as a substitute for lime for microfilling, reducing costs, but not to increase compressive strength. The reductions in strength with pozzolans can be justified as the aggregate pozzolanic performance reducing when its fineness was smaller than the size of the aggregate. In addition, at early stages, the pozzolan had an almost single filler effect, and the greatest increase in the strength by pozzolanic reaction only was clearly observed at 180 and 850 days [53].

In this case, not even the combination of BD with the ash of SCB showed efficiency. In addition to that, as already mentioned, the mixtures in the fresh state showed little cohesion and particle aggregation.

Another important issue is the aggregates/binders' ratio, which was once in the mixtures with brick and ash at a 30/70% ratio, which was tested to assess the possibility of reducing the amount of binder material. However, due the little cohesion observed, a final composition was made with lime and ash only, again with the ratio of the initial compositions of reference 25/75% ratio, and, as shown, the results were better and higher than the reference mixtures only with lime, as mentioned before.

3.3. Thermal Conductivity Test

The comparison of the results between the mixtures shows that the mixtures, based on pozzolans, have the lowest thermal conductivities, confirming the results of Abdellatef's study [54] that added 10% crushed brick to the hempcrete and had the lowest thermal conductivity. As can be seen in Figure 5, the HS25-L-B-A, HS50-L-B-A, and HS75-L-B-A mixtures presented values very close to each other, 0.089 W/m °C on average, while the mixture based only on lime and SCBA was closer to the values obtained for the H-L-ref and HS-L mixtures, around 0.11 W/m °C, whose results were compatible with those found in the literature, between 0.06 and 0.14 W/m °C [54].

These were also comparable with the results of P. Leão and E. Araújo, with a conductivity coefficient of 0.11 and 0.12 W/m °C, with a similar ratio of aggregates/binders (25/75%).

The results obtained from the tests showed that none of the mixtures were within the parameters to be considered conventional thermal insulating materials, according to Portuguese regulations. According to ITE50 [55], an insulation material must have a thermal conductivity lower than 0.065 W/m °C (blue line in Figure 6) and a thermal resistance higher than 0.030 m² °C/W. Regarding thermal resistance, Figure 13 shows that all the mixtures had good thermal resistance, with results above 0.030 m² °C/W (red line in Figure 5), with an average of 0.533 m² °C/W. However, these rules were made for materials only with thermal functions, but the objective of this material was to be used to substitute the set masonry/insulation or other non-structural wall materials that do not need additional insulation. As such, these thermal conductivity values are closer to these materials: aerated concrete (0.16); calcium silicate board (0.17); prefabricated timber wall panels (0.12); and timber blocks (650 kg/m^3) (0.14) [56]. The smaller this value is, the better its behavior is, and it could be considered that the developed composite presented good thermal performance.

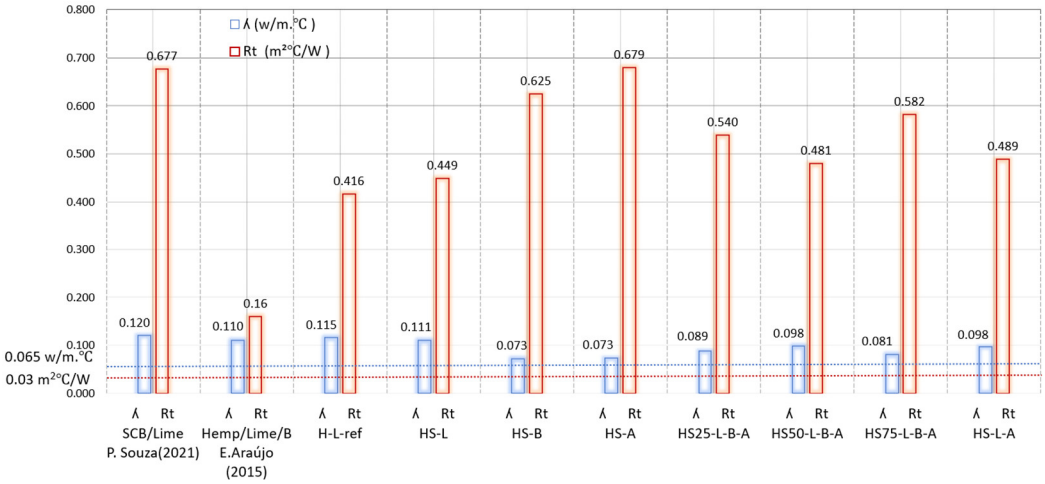

Figure 13. Thermal coefficient ƛ (W/m °C) and thermal resistance Rt (m² °C/W).

3.4. Coefficient of Water Absorption by Capillarity

Figure 14 shows the capillary water absorption coefficients of the mixtures studied. It was observed that the lime-based mixes without pozzolan materials presented the closest coefficients, with an average of 4.78 kg/(m² $h^{0.5}$). In the mixes that were based on the three and two binders, the absorption coefficient decreased by 45.73% when the three binders studied were mixed and only around 30% with the SCBA mixes (HS-A and HS-L-A), with respect to the lime-based mixes.

In the HS25-L-B-A, HS50-L-B-A, HS75-L-B-A, and HS-L-A mixes, the effect of SCBA in combination with lime could be observed, the percentage of water absorption was directly related to the permeability and the porosity of the sample, due to the porosity of the sample, due to the pozzolanic performance of the SCBA, and it had the same effect as in the high-performance concrete, it decreased the water absorption and porosity of the mixes [10]. The added 25% percent of ash could be considered as being effective, as it improved performance by decreasing water absorption. Ganesan et al. used 20% from SCBA also improved the water absorption behavior, due to the formation of a dense microstructure in the mixed concrete from 20% [57].

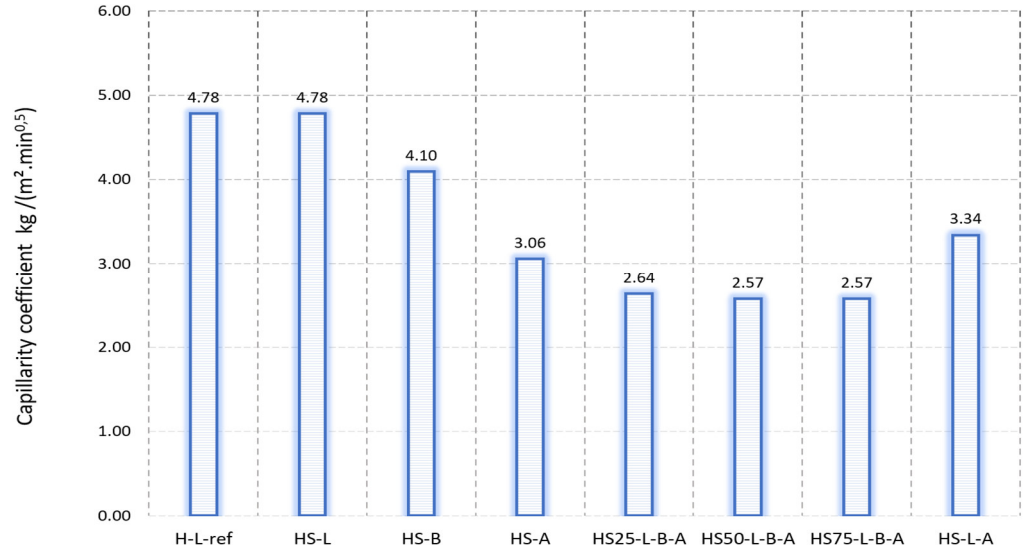

Figure 14. Capillarity absorption coefficient.

Figure 15 shows the behavior of the samples over time, in contact with the water, until stability is reached. HS25-L-B-A, HS50-L-B-A, HS75-L-B-A, and HS-L-A samples

present a linear trend, with an imperceptible variation, achieving stability after 5 √min, while the other mixtures only achieve a linear stability until after 22 √min. This indicates that these mixtures will have a larger open porosity that will facilitate water passage in the early stages of the test.

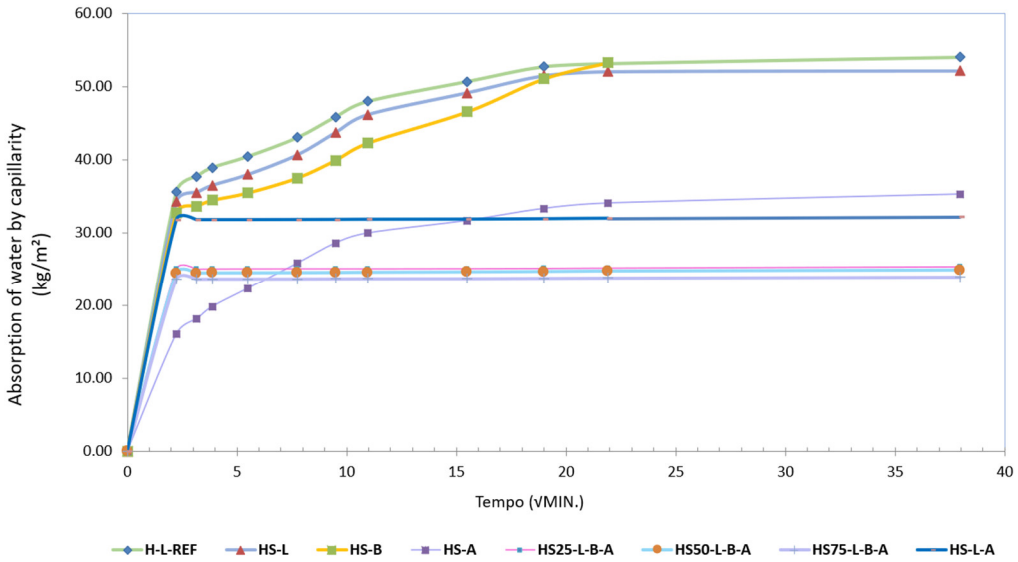

Figure 15. Water absorption by the samples over time.

Concerning the results with brick dust and ash mixtures, although other authors mentioned that the mortar matrix structure only became denser with the formation of the hydration components of pozzolanic activity, decreasing the porosity [53], in this case, the reduced absorption at an early age, also showed a filler effect on the voids. These materials mixes could act as water retainers once with the introduction of small pores that could cut the capillary network [58]. However, for a better understanding of the direct relationship between the absorption and porosity of these composite materials, further tests would have to be carried out, such as absorption by immersion.

3.5. Freezing and Thawing Resistance

For the application of the test, the samples were grouped according to binders. The H-L-ref and HS-L mixtures were subjected to seven freeze–thaw cycles and had a density loss of 8.93% and 6.09%, respectively. The samples showed cracks at the level of visible water absorption, between 25 and 35 mm. The H-L-ref mix was the most damaged, losing its shape and part of the material, while HS-L maintained its dimensions and presented narrower cracks. Both mixtures presented cracks on the upper face and lost the binder at their bases, leaving the aggregates exposed. Figure 16 shows the level of degradation after freeze/thaw cycles of five blends (the beginning—top figure; and the end—bottom figure), completed 30.95 freeze/thaw cycles, and had an average density loss of 2.37%. The HS-A (Figure 17e) blend had the highest density loss (20.47%), reaching the end of the test full of water with completely disintegrated areas. The HS50-L-B-A (Figure 17c) mix presented the lowest loss (1.35%), with a composition of 50% SCB as an aggregate. It can be observed that the sample of the HS-L-A (Figure 17d) mix maintained its dimensions but was completely wetted with a density loss of 1.59%. In general, the mixes maintained their shapes, resisted the cycles, and did not present cracks, but some samples ended up without binder coverage, with exposed fibers or lost part of the material.

(**a**) (**b**) (**c**) (**d**) (**e**)

Figure 16. (**a**) View of HS25-L-B-A. (**b**) View of HS50-L-B-A. (**c**) View of HS75-L-B-A. (**d**) View of HS-L-A. (**e**) View of HS-A.

(**a**) (**b**) (**c**) (**d**)

Figure 17. View of the samples after the rain simulation test, recording the weight gained by the specimens. (**a**) View of H-L-ref. (**b**) View of HS25-L-B-A. (**c**) View of HS50-L-B-A. (**d**) View of HS-B**.**

The HS-B mix performed separately due to its composition. The samples were completely filled with water, and, although they maintained their shape, they had some loss of material.

The addition of SCBA in combination with lime increased the cementitious properties to form hydrated calcium silicate (the pozzolan effects), confirming the study of Botas et al. (2010) [59] on the freeze–thaw resistance of lime mortars. They concluded that the increase in mechanical strength of air lime and hydraulic lime mortars was generally associated with a lower resistance to freeze–thaw cycles due to an increase in porosity, most likely accompanied by a reduction in pore size. Thus, when there was a greater number of pores with smaller dimensions, the performance of mortars against freeze–thaw cycles worsened.

3.6. Degradation by Exposure to Simulated Rain

Table 4 shows the results obtained after the rain-erosion degradation test. In general, the mixes had an average mass loss (ML_r) of 5.35%, except for the HS-D that showed the smallest mass loss (3.78%) and the highest absorption (Ab_r) percentage 42.80%. Regarding flexural behavior, the results (F) are for the mixes that were not subjected to the rain simulation test, with a curing time of 28 days plus the period of 14 days for the application of the finish, in total, 42 days before the flexural test, without being subjected to the rain simulation. The results (Fr) are for the mixes that were subjected to the rain erosion degradation test, with the same curing and finishing time, plus 3 days for the test (time of exposure to water and the drying period until reaching a constant mass), totaling 45 days for all samples before performing the flexural test. Comparing these results, in general, there was no significant difference in the flexural strength, mainly for the mixtures

without ash, but they show a reduction of around 12% in HS75-L-B-A and HS-L-A, as can be seen in Table 4.

Table 4. Results obtained after the rain-erosion degradation test.

Mix	Abr (%)	MLr (%)	Fr (Mpa)	F (Mpa)
H-L-ref	35.39	5.42	0.09	0.09
HS-L	37.00	5.46	0.16	0.17
HS-B	42.80	3.78	0.05	0.04
HS25-L-B-A	9.36	4.84	0.22	0.25
HS50-L-B-A	12.56	6.22	0.26	0.27
HS75-L-B-A	12.50	5.12	0.17	0.24
HS-L-A	8.88	5.06	0.34	0.39

However, it was again verified that ashes decreased the water absorption capacity of the mixes. In general, the new composite, with SCB incorporation, obtained good results when exposed to the rain simulation for a period of 100 years, compatible with the study of Miller's hemp concrete in his life cycle analysis [60], with an average life of more than 100 years. Figure 17 shows an example of the difference in weight gained after the rain simulation test of the different test specimens.

Comparing the HS-L with the hempcrete mixture (HL-ref), there were no significant differences. Nevertheless, the last mixture HS-L-A showed the lowest water absorption, and the loss of mass did not compromise its effectiveness because the value obtained was higher than that of the other mixtures.

3.7. Saline Exposure

The density and compressive strength of the mixtures were evaluated during salt exposure. For density, during the test, the samples did not show large variations, although the trend was that the density increased due to the exposure to moisture.

To evaluate the effect of salt exposure on the samples, Figure 18 shows the results of the mechanical compressive strength tests of the samples in comparison with the results of the samples with 28 days of curing. This improvement in the compressive strength of the mixtures could be attributed to the additional hydration due to the presence of water, as mentioned in the study by Walker et al. (2014) [6]. They used the same temperature and time interval as in the salt exposure test, achieving a significant increase in compressive strength after salt exposure. The authors attributed this increase in additional hydration due to the presence of water and weight gain due to salt crystallization within its pores, suggesting that small pores facilitated salt crystallization.

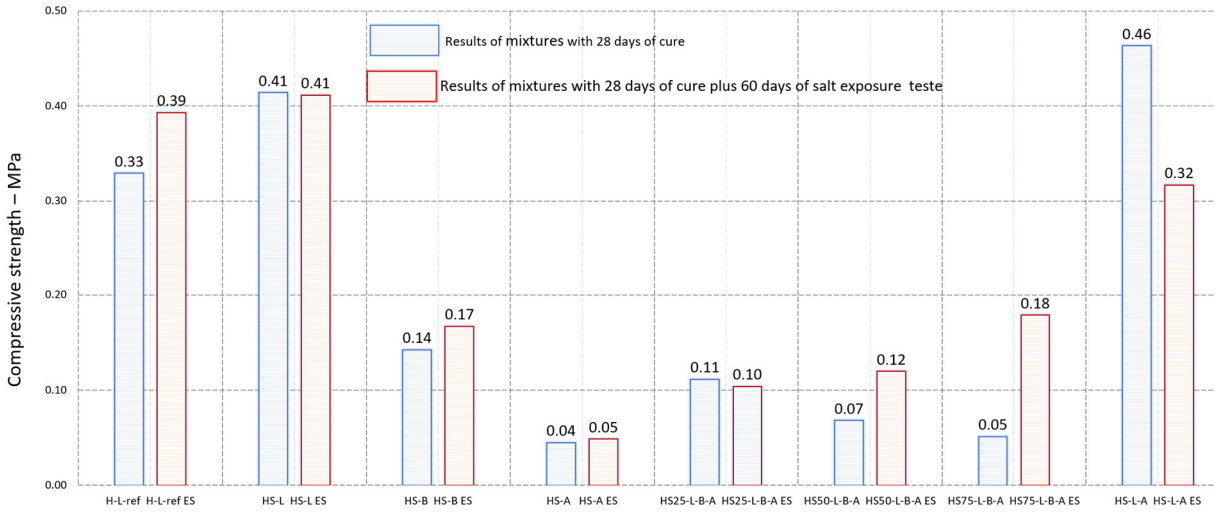

Figure 18. Comparison of compressive strength test with samples exposed to salts.

In the case of the HS-L-A mixture, it presented a loss of 31.66% of its resistance and did not present any change in appearance or visible discoloration. In this composition, the percentage of ashes was higher combined with hydrated lime, and exposure to moisture decreased resistance, otherwise, with the other mixtures.

4. Comparative Analysis of Trials

Table 5 presents a consolidation of all the results, assigning an evaluation from 1 to 8, with 1 being the best result and 8 the worst result, to determine which of the mixtures had the best results in the mechanical and durability tests.

Table 5. Analysis of results by mixtures and tests.

Tests	H-L-ref	HS-L	HS-B	HS-A	HS25-L-B-A	HS50-L-B-A	HS75-L-B-A	HS-L-A
Compressive strength performance	3	2	4	8	5	6	7	1
Thermal coefficient	8	7	1	2	4	6	3	5
Thermal Resistance	8	7	2	1	4	5	3	6
Coefficient of water absorption by capillarity	6	7	5	8	1	3	2	4
Freezing and thawing resistance	6	5	7	8	3	1	4	2
Degradation by exposure to simulated rain (% absorption)	5	6	7	8	2	4	3	1
Degradation by exposure to simulated rain (% erosion wear)	5	6	1	8	2	7	4	3
Degradation by exposure to simulated rain, Flexural strength	6	5	7	8	3	2	4	1
Saline exposure, Compressive strength performance	2	1	5	8	7	6	4	3
Total	49	46	39	59	31	40	34	26
Position	7	6	4	8	2	5	3	1

The mixture with the best performance in the different tests was HS-L-A, with a replacement of hemp by SCB of 25% and also a replacement of lime by SCBA of 25%, with the better results mainly in mechanical performance and in the behavior against environmental agents such as temperature difference and exposure to rain and salts.

It could also be observed that the substitution of hemp by SCB only showed the best results with the addition of SCB ash.

Additionally, considering the results of the mixtures with 25, 50, and 75% of SCB, it was also noted that there was no direct relationship in the results with the percentage of SCB used.

Table 6 shows a comparison of the best performing HS-L-A mixture with some benchmark studies. Although it cannot be directly compared this study, the new composite had good performance, considering that it took two agro-residues and tried to reduce the use of lime.

Table 6. Analysis of results by authors.

Text \ References	(HS-L-A)	[35]	[6]	[21]	[3]	[61]	[62]	[63]
Aggregates/ Binders	SCB/Lime SCBA	SCB/Lime	Hemp/ Lime	Hemp/ Lime	Hemp/ Hydraulic Lime—Pozzolanic Lime	Hemp/ Lime-Based and Natural Cement	Hemp/ Lime-Metakaolin	Hemp/ Lime-
Compressive strength performance	0.46 MPa	0.49 MPa	0.37 MPa	0.6 MPa	0.3 MPa	0.2 MPa	1.64 MPa	0.266 MPa
Thermal coefficient	0.098 W/m °C	0.12 W/m °C		0.11 W/m °C		0.10 to 0.12 W/m °C		
Thermal Resistance	0.48 m² °C/W	0.67 m² °C/W		0.16 m² °C/W				
Coefficient of water absorption by capillarity	3.34 kg/m²	5.26 kg/m²		4.29 kg/m²				
Freezing and thawing resistance	−1.59%/31 cycle		−0.23%/No inf.					
Degradation by exposure to water action Flexural strength, Ft Compressive strength, Fc	0.34 MPa Ft better result with SCBA simulated rain (equivalent of 100 years)					0.2 to 0.5 Fc without significant changes in compressive strength (2 years high humidity/drying cycles)	0.56 MPa Ft flexural strength better results in mixtures with metakaolin (50 wetting/drying cycles)	
Saline exposure, Compressive strength performance	0.32 MPa		0.43 MPa					

The mechanical strength results, compared to the other authors, were within the averages, with better results than Walker et al. (2014) [6], Arnaud Gourlay (2012) [3], and Sinka et al. (2014) [63]. In the case of the other authors, they had additional components to their mixtures such as paper pulp and borax. Comparing the mixture of the new composite with the mixture of only SCB with lime, the results were very close; therefore, it is necessary to analyze its advantages with other parameters that contribute to improve both compositions at the same time.

Within the thermal parameters, the new composite has good performance, with an approximate improvement of 22.44%, even in the case of other materials in the mixtures

such as paper pulp from Eire's study, and the lime- and natural-cement-based mixtures of Delannoy with a coefficient between 0.10 and 12 W/m °C [60]. In the case of Araújo's results, they were evaluated in the form of plates, with a thickness of 0.0173 m, which makes them not very comparable.

In the case of the durability tests, as the Salim study refers to, it is an area with little attention, except for freezing and thawing. The few studies that have analyzed hemp concrete suggest that it works well in most cases, it can be seen that the loss of density in general is low, and, in this study, the loss was higher by 1.36% than Walker et al (2014) [6] study. Thus, the recommendation that hemp concrete should be reinforced against freezing and thawing is valid.

In the salt exposure tests, which were evaluated under the same conditions in both studies, Walker et al (2014) [6] mixtures gained better compressive strengths in some compositions and to a lesser extent in mixtures with SCBA. In this case, as we are comparing as the HS-L-A mixture in this test, it did not perform well and presented a loss of 31.66%. In Walker et al (2014) [6] study, it gained 16.21% performance, and it is an area for further research to check for a trend.

After 50 ageing cycles in Zerrouki's study [62], the compressive strength decreased by 1.35 to 0.35 MPa, corresponding to 26.76% with the metakaolin mix. In this study, the mix HS-L-A that reduce from 0.39 to 0.32 MPa, it had a reduction of only 14.70%, considering that the samples were subjected to degradation by simulated rainfall for 100 years.

5. Conclusions

The mixtures with the best mechanical performance were those with 25% aggregate (H-75%, SCB-25%) and 75% binder. An increase of more than 50% in SCB addition reduced compressive strength, as did a decrease in binder percentage to less than 65%. As well as sugar, bagasse ash significantly increased the compressive strength by almost 40%. This confirms the findings of other studies that a decrease in fiber percentage with an increase in binder improves mechanical strength and that SCBA increases the level of pozzolan in the composition. In addition, there was a reduction of 25% in the amount of hydrated lime used since this percentage was replaced by SCBA, which contributes to the sustainability of the composite.

The incorporation of SCB to hemp concrete (HC) to form a new composite confers new properties that improve durability conditions, but they must be in a percentage range in which the SCB does not exceed 50% in the composition.

The SCBA improved the water absorption performance, which allowed good results after the durability tests, for example, improving the resistance to freeze–thaw cycles by 400% more than HC.

The mixtures have good thermal resistance and conductance, considering the function of this material to other non-structural wall materials. The best performing mixtures were HS-B and HS-A, due to the low density of the samples.

It is worth highlighting the direct benefits, as no additional treatment is applied to this natural aggregate SCB, of agro-industrial waste, highly available from the sugar production process. This can improve the mechanical strength and durability conditions of the widely studied hemp concrete without any additive that was not natural.

The improvement of the durability of this lime-based composite is something that allows building owners and builders to increase their confidence in lime- and plant-based composites. However, for future use, it is considered that this composite still needs to be further studied before to be applied.

It is believed that this composite will be able to be used under the same conditions as hemp concrete, using a rendering for protection against the action of water and reducing water absorption. Structurally, a structural material will be necessary, and this composite could be used as non-structural masonry, in blocks or cast and compacted in situ.

6. Recommendations

For researchers intending to conduct research using this type of material, it is recommended to develop the following topics:

- Develop microscopic studies to better understand the adherence and reactions between the materials.
- Try different percentages of sugar cane bagasse ash.
- Study the effects of other binders, such as hydraulic lime and metakaolin, in combination with SCBA ash.
- Study methods to standardize the compaction process to assess the influence of the compaction process on the mechanical and thermal strength of the mixtures.
- To carry out pre-treatment procedures of sugarcane bagasse ash to reduce the effects of high water absorption and to be able to control the amount of water in the mixture.
- Develop tests with real scale walls with blocks or cast and compacted in situ.

Author Contributions: Writing—original draft, A.Z.; Writing—review and editing, R.E. and R.M. All authors have read and agreed to the published version of the manuscript.

Funding: This research received no external funding.

Data Availability Statement: More data information can be found in the Zúniga Master's Thesis, "Desenvolvimento de compósito à base de cânhamo e bagaço de cana-de-açúcar para blocos construtivos" (In Portuguese) at http://repositorium.sdum.uminho.pt/ (accessed on 22 March 2023).

Conflicts of Interest: The authors declare no conflict of interest.

References

1. Janet, L.S.; Jay, R.; Freyr, S. Renewables 2018-Global Status Report. A Comprehensive Annual Overview of the State of Renewable Energy. Advancing the Global Renewable Energy Transition-Highlights of the REN21 Renewables 2018 Global Status Report in Perspective; 2018. Available online: https://ren21.net/gsr-2018/pages/foreword/foreword/ (accessed on 22 March 2023).
2. Monreal, P.; Mboumba-Mamboundou, L.B.; Dheilly, R.M.; Quéneudec, M. Effects of aggregate coating on the hygral properties of lignocellulosic composites. *Cem. Concr. Compos.* **2011**, *33*, 301–308. https://doi.org/10.1016/j.cemconcomp.2010.10.017.
3. Arnaud, L.; Gourlay, E. Experimental study of parameters influencing mechanical properties of hemp concretes. *Constr. Build. Mater.* **2012**, *28*, 50–56. https://doi.org/10.1016/j.conbuildmat.2011.07.052.
4. Barbhuiya, S.; Bhusan Das, B. A comprehensive review on the use of hemp in concrete. *Constr. Build. Mater.* **2022**, *341*, 127857. https://doi.org/10.1016/j.conbuildmat.2022.127857.
5. Jami, T.; Karade, S.R.; Singh, L.P. A review of the properties of hemp concrete for green building applications. *J. Clean. Prod.* **2019**, *239*, 117852. https://doi.org/10.1016/j.jclepro.2019.117852.
6. Walker, R.; Pavia, S.; Mitchell, R. Mechanical properties and durability of hemp-lime concretes. *Constr. Build. Mater.* **2014**, *61*, 340–348. https://doi.org/10.1016/j.conbuildmat.2014.02.065.
7. Nozahic, V.; Amziane, S.; Torrent, G.; Saïdi, K.; Baynast, H. De Design of green concrete made of plant-derived aggregates and a pumice—Lime binder. *Cem. Concr. Compos.* **2012**, *34*, 231–241. https://doi.org/10.1016/j.cemconcomp.2011.09.002.
8. Chabannes, M.; Nozahic, V.; Amziane, S. Design and multi-physical properties of a new insulating concrete using sunflower stem aggregates and eco-friendly binders. *Mater. Struct. Constr.* **2015**, *48*, 1815–1829. https://doi.org/10.1617/s11527-014-0276-9.
9. Chabannes, M.; Bénézet, J.; Clerc, L.; Garcia-diaz, E. Use of raw rice husk as natural aggregate in a lightweight insulating concrete : An innovative application. *Constr. Build. Mater.* **2014**, *70*, 428–438. https://doi.org/10.1016/j.conbuildmat.2014.07.025.
10. Ntimugura, F.; Vinai, R.; Harper, A.B.; Walker, P. Environmental performance of miscanthus-lime lightweight concrete using life cycle assessment : Application in external wall assemblies. *Sustain. Mater. Technol.* **2021**, *28*, e00253. https://doi.org/10.1016/j.susmat.2021.e00253.
11. Garikapati, K.P.; Sadeghian, P. Physical and Mechanical Properties of Flax Lime Concrete. 2018. Conferência Anual da CSCE Em: Fredericton, NB, Canadá. Available online: https://www.researchgate.net/publication/325949496 (accessed on 14 April 2023).
12. Brzyski, P.; Barnat-Hunek, D.; Suchorab, Z.; Łagód, G. Composite Materials Based on Hemp and. *Flax Low-Energy Build. Mater.* **2017**, *10*, 510. https://doi.org/10.3390/ma10050510.
13. Kumar, N.; Barbato, M. Effects of sugarcane bagasse fibers on the properties of compressed and stabilized earth blocks. *Constr. Build. Mater.* **2022**, *315*, 125552. https://doi.org/10.1016/j.conbuildmat.2021.125552.
14. Lavarack, B.P.; Griffin, G.J.; Rodman, D. Measured kinetics of the acid-catalyzed hydrolysis of sugar cane bagasse to produce xylose. *Catal. Today* **2000**, *63*, 257–265. https://doi.org/10.1016/S0920-5861(00)00467-3.
15. Salih, M.M.; Osofero, A.I.; Imbabi, M.S. Constitutive models for fibre reinforced soil bricks. *Constr. Build. Mater.* **2020**, *240*,

117806. https://doi.org/10.1016/j.conbuildmat.2019.117806.
16. Dineshkumar, R.; Balamurugan, P. Behavior of high-strength concrete with sugarcane bagasse ash as replacement for cement. *Innov. Infrastruct. Solut.* **2021**, *6*, 63. https://doi.org/10.1007/s41062-020-00450-4.
17. Katare, V.D.; Madurwar, M.V. Process standardization of sugarcane bagasse ash to develop durable high-volume ash concrete. *J. Build. Eng.* **2021**, *39*, 102151. https://doi.org/10.1016/j.jobe.2021.102151.
18. Kazmi, S.M.S.; Abbas, S.; Saleem, M.A.; Munir, M.J.; Khitab, A. Manufacturing of sustainable clay bricks: Utilization of waste sugarcane bagasse and rice husk ashes. *Constr. Build. Mater.* **2016**, *120*, 29–41. https://doi.org/10.1016/j.conbuildmat.2016.05.084.
19. Nancy, T.; Hussien, A.F.O. The use of sugarcane wastes in concrete. *J. Eng. Appl. Sci.* **2022**, 4–9 https://doi.org/10.1186/s44147-022-00076-6.
20. Berenguer, R.; Lima, N.; Valdés, A.C.; Medeiros, M.H.F.; Lima, N.B.D.; Delgado, J.M.P.Q.; Silva, F.A.N.; Azevedo, A.C.; Guimarães, A.S.; Rangel, B. Durability of Concrete Structures with Sugar Cane Bagasse Ash. *Adv. Mater. Sci. Eng.* **2020**, *2020*, 6907834. https://doi.org/10.1155/2020/6907834.
21. Athira, V.S.; Charitha, V.; Athira, G.; Bahurudeen, A. Agro-waste ash based alkali-activated binder: Cleaner production of zero cement concrete for construction. *J. Clean. Prod.* **2021**, *286*, 125429. https://doi.org/10.1016/j.jclepro.2020.125429.
22. Murphy, F.; Pavia, S.; Walker, R. An Assessment of the physical properties of lime-hemp concrete. Proc. of BRI/CRI. Ní Nualláin, Walsh, West, Cannon, Caprani, McCabe eds. Cork 2010 Dept. of Civil Engineering, Trinity College, Dublin, Ireland. **2010**, *2*, 431–439. Available online: https://www.researchgate.net/publication/235641051 (accessed on 22 March 2023).
23. Araújo, E.F. Materiais Compósitos com Incorporação de Cânhamo Industrial. Master's Thesis, University of Minho, Braga, Portugal, 2015. Available online: https://hdl.handle.net/1822/40358 (accessed on 22 March 2023).
24. Atlas Big Los principales países productores de caña de azúcar del mundo Países. 2020. 2021–2022. Available online: https://www.atlasbig.com/es-mx/paises-por-produccion-de-cana-de-azucar (accessed on 22 March 2023).
25. Food and Agriculture Organization of the United Nations, Perspectivas agrícolas OCDE-FAO 2020–2029 FAO Perspectivas agrícolas. FAO 2020. Available online: https://www.fao.org/3/ca8861es/ca8861es.pdf (accessed on 22 March 2023).
26. United States Department of Agriculture, 2017 census of agriculture: Louisiana; United States Dep, Agric, 2019. Louisiana State and Parish Data 2019, 1. Available online: https://www.nass.usda.gov/Publications/AgCensus/2017/Full_Report/Volume_1,_Chapter_1_US/usv1.pdf (accessed on 22 March 2023).
27. CNPA NIC. 2021–2022 Comité Nacional de Produtores de Azucar de Nicaragua, Datos Finales de Producción Zafra 2021–2022 Zafra 2021/22. Available online: https://cnpa.com.ni/wp-content/uploads/2022/06/Nic_Zafra-21-22S.pdf (accessed on 22 March 2023).
28. Products, H.V. Lignocellulosic Materials for Production of Cement Composites : Valorization of the Alkali Treated Soybean Pod and Eucalyptus Wood Particles to Obtain Lignocellulosic Materials for Production of Cement Composites : Valorization of the Alkali Treated Soybean Pod and Eucalyptus Wood Particles to Obtain Higher Value-Added Products. *Waste Biomass Valorization* **2020**. https://doi.org/10.1007/s12649-018-0488-2.
29. Karade, S.R. Cement-bonded composites from lignocellulosic wastes. *Constr. Build. Mater.* **2010**, *24*, 1323–1330. https://doi.org/10.1016/j.conbuildmat.2010.02.003.
30. Beskopylny, A.N.; Shcherban, E.M.; Stel, S.A.; Meskhi, B.; Shilov, A.A.; Varavka, V.; Evtushenko, A.; Özkılıç, Y.O.; Aksoylu, C.; Karalar, M. Composition Component Influence on Concrete Properties with the Additive of Rubber Tree Seed Shells. *Appl. Sci.* **2022**, *12*, 11744.
31. Shcherban, E.M.; Stel, S.A.; Beskopylny, A.N.; Mailyan, L.R.; Meskhi, B.; Shilov, A.A.; Chernil, A.; Özkılıç, Y.O.; Aksoylu, C. Normal-Weight Concrete with Improved Stress—Strain Characteristics Reinforced with Dispersed Coconut Fibers. *Appl. Sci.* **2022**, *12*, 11734.
32. Ferraz, P.; Mendes, R.F.; Marin, D.B.; Paes, J.L.; Cecchin, D.; Barbari, M. Agricultural Residues of Lignocellulosic Materials in Cement Composites. *Appl. Sci.* **2020**, *10*, 8019.
33. Bock-Hyeng, C.; Ofori-Boadu, A.N.; Yamb-Bell, E.; Shofoluwe, M.A. Mechanical Properties of Sustainable Adobe Bricks Stabilized With Recycled Sugarcane Fiber Waste. *Int. J. Eng. Res. Appl.* **2016**, *6*, 50–59.
34. Lee, S.C.; Mariatti, M. The effect of bagasse fibers obtained (from rind and pith component) on the properties of unsaturated polyester composites. *Mater. Lett.* **2008**, *62*, 2253–2256. https://doi.org/10.1016/j.matlet.2007.11.097.
35. Memon, S.A.; Wahid, I.; Khan, M.K.; Tanoli, M.A.; Bimaganbetova, M. Environmentally friendly utilization of wheat straw ash in cement-based composites. *Sustainability* **2018**, *10*, 1322. https://doi.org/10.3390/su10051322.
36. Charitha, V.; Athira, V.S.; Jittin, V.; Bahurudeen, A.; Nanthagopalan, P. Use of different agro-waste ashes in concrete for effective upcycling of locally available resources. *Constr. Build. Mater.* **2021**, *285*, 122851. https://doi.org/10.1016/j.conbuildmat.2021.122851.
37. Sousa, P. L Compósitos de Bagaço de Cana-de-Açúcar para Blocos Construtivos. Master's Thesis, University of Minho, Portugal, 2021. Available online: https://hdl.handle.net/1822/75869 (accessed on 22 March 2023). (In Portuguese)
38. Bahurudeen, A.; Santhanam, M. Performance evaluation of sugarcane bagasse ash-based cement for durable concrete. In Proceedings of the 4th International Conference on the Durability of Concrete Structures, ICDCS 2014, Madrid, Spain, 30 June–3 July 2014; pp. 275–281.
39. Zúniga, Arlen, L.G. Desenvolvimento de compósito à base de cânhamo e bagaço de cana-de-açúcar para blocos construtivos. Master's Thesis, University of Minho, Portugal, 2022. (In Portuguese)

40. Elfordy, S.; Lucas, F.; Tancret, F.; Scudeller, Y.; Goudet, L. Mechanical and thermal properties of lime and hemp concrete ("hempcrete") manufactured by a spraying process. *Constr. Construir. Mater.* **2008**, *22*, 2116–2123.
41. CEN—European Committee for Standardization. *EN 1015-11*; Methods of Test for Mortar for Masonry EN 1015-11:1999. Part 11 Determ. Flexural Compressive Strength Hardened Mortar. CEN: Brussels, Belgium, 2006; Volume 3.
42. Gomes, F.; Rute, M.G.; Eires Raúl, M.E. Sousa Fangueiro Placas à base de Desperdícios Industriais para paredes Interiores. Master's Thesis, Universidade do Minho, Braga, Portugal, 2021.
43. CEN—European Committee for Standardization. *ISO 9869*; Thermal Insulation—Building Elements—In-Situ Measurement of Thermal Resistance and Thermal Transmittance. CEN: Brussels, Belgium, 1994; Volume 994, p. 32.
44. *BS EN 1015-18:2002*; Methods of test for mortar for masonry. Determination of water absorption coefficient due to capillary action of hardened mortar. British Standard Institution: London, UK, 2002.
45. ASTM-American Society for Testing and Materials. *ASTM C 1585 04*; Standard Test Method for Measurement of Rate of Absorption of Water by Hydraulic-Cement Concretes. ASTM: West Conshohocken, PA, USA, 2007; pp. 1–6.
46. ASTM-American Society for Testing and Materials. *ASTM C666/C666M*; Standard Test Method for Resistance of Concrete to Rapid Freezing and Thawing. ASTM Int.: West Conshohocken, PA, USA, 2003; Volume *3*, pp. 1–6.
47. Rezende, M.L.; Camões, A.; Eires, R.; Jesus, C.M.G.; Soares, E. Proposta de Ensaio Acelerado de Exposição a Chuvas Dirigidas (in English—Proposal of Accelerated Test Exposure To Driving Rain), TEST&E 2019, 2° Congresso de Ensaios e Experimentação em Engenharia Civil, 2019. Available online: https://hdl.handle.net/1822/63248 (accessed on 22 March 2023). (In Portuguese)
48. British Standard. *BS 3900-0:2010*; Standards Publication Methods of test for paints—Part 0: Index of test methods. Third revision, May 2010. BSI: London, UK, 2010.
49. Eires, R.M.G. Materiais Não Convencionais para uma Construção Sustentável Utilizando Cânhamo, Pasta de Papel e Cortiça. Master's Thesis, University of Minho, Portugal. Available online: https://hdl.handle.net/1822/70532006, 125 (accessed on 22 March 2023). (In Portuguese)
50. Benfratello, S.; Capitano, C.; Peri, G.; Rizzo, G.; Scaccianoce, G.; Sorrentino, G. Thermal and structural properties of a hemp-lime biocomposite. *Constr. Build. Mater.* **2013**, *48*, 745–754. https://doi.org/10.1016/j.conbuildmat.2013.07.096.
51. Kasaniya, M.; Alaibani, A.; Thomas, M.D.A.; Riding, K.A. Exploring the efficacy of emerging reactivity tests in screening pozzolanic materials. *Constr. Build. Mater.* **2022**, *325*, 126781. https://doi.org/10.1016/j.conbuildmat.2022.126781.
52. Sinka, M.; Sahmenko, G. Sustainable-thermal-insulation-biocomposites-from-locally-available-hemp-and-lime. In *Environment Technology Resources, Proceedings of the International Scientific and Practical Conference, Rēzekne, Latvia, 20–22 June 2013*; Rēzeknes Augstskola: Rēzekne, Latvia, 2013; pp. 73–77.
53. Su-cadirci, T.B.; Ball, R.J.; Calabria-holley, J. Use of brick dust to optimise the dewatering process of hydrated lime mortars for conservation applications. *Mater. Struct.* **2023**, *56*, 1–19. https://doi.org/10.1617/s11527-023-02128-6.
54. Abdellatef, Y.; Khan, M.A.; Khan, A.; Alam, M.I.; Kavgic, M. Mechanical, thermal, and moisture buffering properties of novel insulating hemp-lime composite building materials. *Materials* **2020**, *13*, 5000. https://doi.org/10.3390/ma13215000.
55. LNEC—Laboratório Nacional de Engenharia Civil. ITE50—Thermal transmission coefficients of building envelope elements. Available online: www.lnec.pt (accessed on 22 March 2023).
56. Press, S.; Park, M. *Ebook Set Up and Use Instructions;* Routledge & CRC Press Spon Press: Abingdon; UK. ISBN 9780367271084.
57. Ganesan, K.; Rajagopal, K.; Thangavel, K. Evaluation of bagasse ash as supplementary cementitious material. *Cem. Concr. Compos.* **2007**, *29*, 515–524. https://doi.org/10.1016/j.cemconcomp.2007.03.001.
58. Walker, R.; Pavía, S. Moisture transfer and thermal properties of hemp—Lime concretes. *Constr. Build. Mater.* **2014**, *64*, 270–276. https://doi.org/10.1016/j.conbuildmat.2014.04.081.
59. Botas, S.M.S.; Rato, V.M.; Faria, P. Testing the Freeze/Thaw Cycles in Lime Mortar. In Proceedings of the 2nd Historic Mortars Conference—HMC 2010 and RILEM TC 203-RHM Final Workshop, Prague, Czech Republic, 22–24 September 2010; pp. 417–425.
60. Ip, K.; Miller, A. Life cycle greenhouse gas emissions of hemp-lime wall constructions in the UK. *Resour. Conserv. Recycl.* **2012**, *69*, 1–9. https://doi.org/10.1016/j.resconrec.2012.09.001.
61. Delannoy, G.; Marceau, S.; Glé, P.; Gourlay, E.; Guéguen-Minerbe, M.; Amziane, S.; Farcas, F. Durability of hemp concretes exposed to accelerated environmental aging. *Constr. Build. Mater.* **2020**, *252*, 119043. https://doi.org/10.1016/j.conbuildmat.2020.119043.
62. Zerrouki, R.; Benazzouk, A.; Courty, M.; Ben, H. Potential use of matakaolin as a partial replacement of preformulated lime binder to improve durability of hemp concrete under cyclic wetting / drying aging. *Constr. Build. Mater.* **2022**, *333*, 127389. https://doi.org/10.1016/j.conbuildmat.2022.127389.
63. Sinka, M.; Korjakins, A. Mechanical Properties of Pre-Compressed Hemp-Lime Concrete. 2014. Available online: https://www.researchgate.net/publication/287503987_ (accessed on 22 March 2023).